Probabilistic Engineering Mechanics 25 (2010) 9–17

Contents lists available at ScienceDirect

Probabilistic Engineering Mechanics

journal homepage: www.elsevier.com/locate/probengmech

Closed-form solutions for the time-variant spectral characteristics of non-stationary random processes

Michele Barbato [a,*], Marcello Vasta [b]

[a] Department of Civil and Environmental Engineering, Louisiana State University, 3531 Patrick F. Taylor Hall, Baton Rouge, LA, 70803, USA
[b] PRICOS, University of Chieti-Pescara "G. D'Annunzio", Viale Pindaro 42, Pescara, 65127, Italy

ARTICLE INFO

Article history:
Received 26 September 2008
Received in revised form
11 May 2009
Accepted 19 May 2009
Available online 27 May 2009

Keywords:
Stationary and non-stationary stochastic processes
Bandwidth parameter
Non-geometric spectral characteristics
Classically and non-classically damped MDOF systems

ABSTRACT

Spectral characteristics are important quantities in describing stationary and non-stationary random processes. In this paper, the spectral characteristics for complex-valued random processes are evaluated and closed-form solutions for the time-variant statistics of the response of linear single-degree-of-freedom (*SDOF*) and both classically and non-classically damped multi-degree-of-freedom (*MDOF*) systems subjected to modulated Gaussian colored noise are obtained. The time-variant central frequency and bandwidth parameter of the response processes of linear *SDOF* and *MDOF* elastic systems subjected to Gaussian colored noise excitation are computed exactly in closed-form. These quantities are useful in problems which require the use of complex modal analysis, such as random vibrations of non-classically damped *MDOF* linear structures, and in structural reliability applications. Monte Carlo simulation has been used to confirm the validity of the proposed solutions.

1. Introduction

The dynamic behavior of structural and mechanical systems subjected to uncertain dynamic excitations can be described, in general, through random processes. The probabilistic characterization of these random processes can be extremely complex, when non-stationary and/or non-Gaussian input processes are involved. In specific applications, an incomplete description of stochastic processes corresponding to dynamic structural response may suffice, based on the spectral characteristics of the processes under study [1,2]. For stationary stochastic processes, the spectral characteristics are defined as the geometric spectral moments of their power spectral density (*PSD*) function [1,2]. On the other hand, the so-called non-geometric spectral characteristics (*NGSCs*) [3–5] can be employed to evaluate the time-variant central frequency and bandwidth parameters, which characterize in a synthetic way a non-stationary stochastic process (*NSSP*). The *NGSCs* have been proved appropriate for describing *NSSPs* and can be effectively employed in structural reliability applications, such as the computation of the time-variant probability that a random process outcrosses a given limit-state threshold [6]. In this paper, using the definition of *NGSCs* for general complex-valued *NSSPs* and complex modal analysis proposed in [5], closed-form solutions for the *NGSCs* of *NSSPs* representing the response of linear elastic structural models subjected to time-modulated colored noises are obtained. It is noteworthy that, while closed-form solutions have been available for more than two decades for the simpler case of geometric spectral moments of stationary stochastic processes [7,8], closed-form solutions for the *NGSCs* of non-stationary response processes of linear systems are very recent for the case of time-modulated white noise inputs [5] and, to the authors' knowledge, are presented in this paper for the first time for the case of time-modulated colored noise inputs. These *NGSCs* are used in this study to compute exactly and in closed-form the time-variant central frequency and bandwidth parameter of the response processes of single-degree-of-freedom (*SDOF*) and both classically and non-classically damped multidegree-of-freedom (*MDOF*) linear elastic systems subjected to colored noise excitation from at rest initial conditions. These closed-form solutions are useful in problems which require the use of complex modal analysis, such as random vibrations of non-classically damped *MDOF* linear structures, and in structural reliability applications [9,10]. For the sake of simplicity and without loss of generality, all random processes considered in this study are zero-mean processes. For these processes, the auto- and cross-covariance functions coincide with their auto- and cross-correlation functions, respectively.

* Corresponding author. Tel.: +1 225 578 8719; fax: +1 225 578 4945.
E-mail addresses: mbarbato@lsu.edu (M. Barbato), m.vasta@unich.it (M. Vasta).

0266-8920/$ – see front matter © 2009 Elsevier Ltd. All rights reserved.
doi:10.1016/j.probengmech.2009.05.002

2. Central frequency and bandwidth parameters of non-stationary stochastic processes

A non-stationary stochastic process (*NSSP*) $X(t)$ can be expressed in the general form of a Fourier–Stieltjes integral as [1]

$$X(t) = \int_{-\infty}^{\infty} A_X(\omega, t) e^{j\omega t} dZ(\omega) \tag{1}$$

in which t = time, ω = frequency parameter, $j = \sqrt{-1}$, $A_X(\omega, t)$ = complex-valued deterministic time–frequency modulating function and $dZ(\omega)$ = zero-mean orthogonal-increment process defined so that $E[dZ^*(\omega_1)dZ(\omega_2)] = \Phi(\omega_1)\delta(\omega_1 - \omega_2)d\omega_1 d\omega_2$, where $E[\cdot]$ = mathematical expectation, $\Phi(\omega) = PSD$ function of the embedded stationary process $X_S(t)$, $\delta(\cdot)$ = Dirac delta function and the superscript $(\cdot)^*$ denotes the complex-conjugate operator. The process $X(t)$ has the following evolutionary power spectral density (*EPSD*) function:

$$\Phi_{XX}(\omega, t) = A_X^*(\omega, t)\Phi(\omega)A_X(\omega, t). \tag{2}$$

It is also convenient to define the process $Y(t)$ as the modulation (with modulating function $A_X(\omega, t)$) of the stationary process $Y_S(t)$ defined as the Hilbert transform of the embedded stationary process $X_S(t)$ [11,12], i.e.,

$$Y(t) = -j \int_{-\infty}^{\infty} \mathrm{sign}(\omega) A_X(\omega, t) e^{j\omega t} dZ(\omega). \tag{3}$$

For each *NSSP* $X(t)$, two sets of non-geometric spectral characteristics (*NGSCs*) can be defined as follows [5]

$$\begin{cases} c_{ik,XX}(t) = \displaystyle\int_{-\infty}^{\infty} \Phi_{X^{(i)}X^{(k)}}(\omega, t) d\omega = \sigma_{X^{(i)}X^{(k)}}(t) \\ c_{ik,XY}(t) = \displaystyle\int_{-\infty}^{\infty} \Phi_{X^{(i)}Y^{(k)}}(\omega, t) d\omega = \sigma_{X^{(i)}Y^{(k)}}(t) \end{cases} \tag{4}$$

where $\sigma_{X^{(i)}X^{(k)}}(t)$ = cross-covariance of random processes $X^{(i)}(t)$ and $X^{(k)}(t)$, and $\sigma_{X^{(i)}Y^{(k)}}(t)$ = cross-covariance of random processes $X^{(i)}(t)$ and $Y^{(k)}(t)$, in which

$$W^{(m)}(t) = \frac{d^m W(t)}{dt^m}, \quad W = X, Y;\ m = i, k. \tag{5}$$

The evolutionary cross-*PSD* functions $\Phi_{X^{(i)}W^{(k)}}(\omega, t)$ ($W = X, Y$ and $i, k = 0, 1, \ldots$) are given by

$$\Phi_{X^{(i)}W^{(k)}}(\omega, t) = A^*_{X^{(i)}}(\omega, t)\Phi(\omega)A_{W^{(k)}}(\omega, t) \tag{6}$$

where [13]

$$A_{W^{(i)}}(\omega, t) = e^{-j\omega t} \frac{\partial^i}{\partial t^i}[A_W(\omega, t)e^{j\omega t}]. \tag{7}$$

Herein, it is assumed that the time-derivative processes in Eq. (4) exist in the mean-square sense. In the particular case when $i = k = n$, the cross-covariance in Eq. $(4)_1$ reduces to the variance of the nth time-derivative of the process $X(t)$, i.e., $\sigma_{X^{(n)}X^{(n)}}(t) = \sigma^2_{X^{(n)}}(t)$.

The four *NGSCs* $c_{00,XX}(t)$, $c_{11,XX}(t)$, $c_{01,XX}(t)$ and $c_{01,XY}(t)$ are particularly relevant to random vibration theory and time-variant reliability applications. In fact, $c_{00,XX}(t)$ and $c_{11,XX}(t)$ represent the variance of the process and its first time-derivative (i.e., $\sigma^2_X(t)$ and $\sigma^2_{\dot{X}}(t)$), respectively, $c_{01,XX}(t)$ denotes the cross-covariance of the process and its first time derivative (i.e., $\sigma_{X\dot{X}}(t)$), and $c_{01,XY}(t)$ represents the cross-covariance of the process $X(t)$ and the first time-derivative of the process $Y(t)$ (i.e., $\sigma_{X\dot{Y}}(t)$). Notice that the definitions in Eq. (5) for $c_{00,XX}(t)$, $c_{11,XX}(t)$, $c_{01,XX}(t)$ and $c_{01,XY}(t)$ are valid for both real-valued and complex-valued *NSSPs* [5]. In the case of real-valued *NSSPs*, these definitions are equivalent to the one proposed in [3,4]. The *NGSCs* $c_{00,XX}(t)$, $c_{11,XX}(t)$ and $c_{01,XY}(t)$ are used in the definition of the time-variant central frequency, $\omega_c(t)$, and bandwidth parameter, $q(t)$, of the *NSSP* $X(t)$ as [5]

$$\omega_c(t) = \frac{c_{01,XY}(t)}{c_{00,XX}(t)} = \frac{\sigma_{X\dot{Y}}(t)}{\sigma^2_X(t)} \tag{8}$$

$$q(t) = \left(1 - \frac{c^2_{01,XY}(t)}{c_{00,XX}(t)c_{11,XX}(t)}\right)^{1/2} = \left(1 - \frac{\sigma^2_{X\dot{Y}}(t)}{\sigma^2_X(t)\sigma^2_{\dot{X}}(t)}\right)^{1/2}. \tag{9}$$

The time-variant central frequency and bandwidth parameter are useful in describing the time-variant spectral properties of a real-valued *NSSP* $X(t)$. The central frequency $\omega_c(t)$ provides the characteristic/predominant frequency of the process at each instant of time. The bandwidth parameter $q(t)$ provides information on the spectral bandwidth of the process at each instant of time. Notice that a *NSSP* can behave as a narrowband and a broadband process at different instants of time. For complex-valued *NSSPs*, the complex-valued central frequency and bandwidth parameter defined in Eqs. (8) and (9) lose the simple physical interpretation available for real-valued *NSSPs*, even though their computation is instrumental to the solution of problems requiring a state-space representation. In addition, the bandwidth parameter $q(t)$ plays an important role in time-variant reliability analysis, since it is an essential ingredient of analytical approximations to the time-variant failure probability for the first-passage reliability problem [9,10,13–17].

3. Spectral characteristics of the stochastic response of SDOF/MDOF linear system subjected to non-stationary excitations

3.1. Complex modal analysis

A state-space formulation of the equations of motion for a linear *MDOF* system is useful to describe the response of both classically and non-classically damped systems [18]. The general (second-order) equations of motion for an n-degree-of-freedom linear system are, in matrix form,

$$\mathbf{M}\ddot{\mathbf{U}} + \mathbf{C}\dot{\mathbf{U}} + \mathbf{K}\mathbf{U} = \mathbf{P}F(t) \tag{10}$$

where $\mathbf{M}$, $\mathbf{C}$, and $\mathbf{K}$ = $n \times n$ time-invariant mass, damping and stiffness matrices, respectively; $\mathbf{U}(t)$ = length-n vector of nodal displacements, $\mathbf{P}$ = length-n load distribution vector, $F(t)$ = scalar function describing the time-history of the external loading (random process), and a superposed dot denotes differentiation with respect to time. The matrix equation of motion Eq. (10) can be recast into the following first-order matrix equation

$$\dot{\mathbf{Z}} = \mathbf{G}\mathbf{Z} + \tilde{\mathbf{P}}F(t) \tag{11}$$

where

$$\mathbf{Z} = \begin{bmatrix} \mathbf{U} \\ \dot{\mathbf{U}} \end{bmatrix}_{(2n\times 1)} \tag{12}$$

$$\mathbf{G} = \begin{bmatrix} \mathbf{0}_{n\times n} & \mathbf{I}_{n\times n} \\ -\mathbf{M}^{-1}\mathbf{K} & -\mathbf{M}^{-1}\mathbf{C} \end{bmatrix}_{(2n\times 2n)} \tag{13}$$

$$\tilde{\mathbf{P}} = \begin{bmatrix} \mathbf{0}_{n\times 1} \\ \mathbf{M}^{-1}\mathbf{P} \end{bmatrix}_{(2n\times 1)}. \tag{14}$$

The subscripts in Eqs. (12)–(14) indicate the dimensions of the vectors and matrices to which they are attached. Using the complex modal matrix $\mathbf{T}$ formed from the complex eigenmodes of matrix $\mathbf{G}$, the first-order matrix equation Eq. (11) can be decoupled into the following $2n$ normalized complex modal equations

$$\dot{S}_i(t) = \lambda_i S_i(t) + F(t), \quad i = 1, 2, \ldots, 2n \tag{15}$$

where $\mathbf{S} = [S_1(t)S_2(t)\cdots S_{2n}(t)]^T$ = normalized complex modal response vector, λ_i ($i = 1, \ldots, 2n$) = complex eigenvalues of the system matrix $\mathbf{G}$, and the superscript $(\cdot)^T$ denotes the matrix transpose operator. The response of the linear *MDOF* system can be obtained as

$$\mathbf{Z}(t) = \mathbf{T}\boldsymbol{\Gamma}\mathbf{S}(t) = \tilde{\mathbf{T}}\mathbf{S}(t) \tag{16}$$

in which $\boldsymbol{\Gamma}$ = diagonal matrix containing the $2n$ modal participation factors Γ_i, defined as the ith component of vector $\mathbf{T}^{-1}\tilde{\mathbf{P}} = [\Gamma_1 \Gamma_2 \cdots \Gamma_{2n}]^{\mathrm{T}}$, and $\tilde{\mathbf{T}} = \mathbf{T}\boldsymbol{\Gamma}$ = effective modal participation matrix. Assuming that the system is initially at rest, the solution of Eq. (15) can be expressed by the following Duhamel integral:

$$S_i(t) = \int_0^t \mathrm{e}^{\lambda_i(t-\tau)} F(\tau)\mathrm{d}\tau, \quad i = 1, 2, \ldots, 2n. \tag{17}$$

It is worth mentioning that the normalized complex modal responses $S_i(t)$, $i = 1, 2, \ldots, 2n$, are complex conjugate by pairs. In the case of a non-stationary loading process, the loading function $F(t)$ can be expressed in general as (see Eq. (1))

$$F(t) = \int_{-\infty}^{\infty} A_F(\omega, t)\mathrm{e}^{\mathrm{j}\omega t}\mathrm{d}Z(\omega). \tag{18}$$

It can be shown that the normalized complex modal responses are given by

$$S_i(t) = \int_{-\infty}^{\infty} A_{S_i}(\omega, t)\mathrm{e}^{\mathrm{j}\omega t}\mathrm{d}Z(\omega), \quad i = 1, 2, \ldots, 2n \tag{19}$$

where

$$A_{S_i}(\omega, t) = \int_{-\infty}^{t} \mathrm{e}^{(\lambda_i - \mathrm{j}\omega)(t-\tau)} A_F(\omega, \tau)\mathrm{d}\tau, \quad i = 1, 2, \ldots, 2n. \tag{20}$$

3.2. NGSCs of response processes of linear MDOF systems using complex modal analysis

The state-space formulation of the equations of motion is also advantageous for the computation of the *NGSCs* of response processes of both classically and non-classically damped linear *MDOF* systems. If only Gaussian input processes are considered, only few spectral characteristics are needed to fully describe the response processes of linear elastic *MDOF* systems, since the response processes are also Gaussian. In particular, if $U_i(t)$ denotes the ith *DOF* displacement response process of a linear elastic *MDOF* system subjected to Gaussian excitation, the only spectral characteristics required, e.g., for reliability applications, are ($i = 1, 2, \ldots, n$)

$$\begin{cases} c_{00,U_iU_i}(t) = \sigma^2_{U_i}(t) \\ c_{11,U_iU_i}(t) = \sigma^2_{\dot{U}_i}(t) \\ c_{01,U_iU_i}(t) = \sigma_{U_i\dot{U}_i}(t) \\ c_{01,U_i\mathcal{Y}_i}(t) = \sigma_{U_i\dot{\mathcal{Y}}_i}(t) \end{cases} \tag{21}$$

where $\dot{\mathcal{Y}}_i$ is the first time-derivative of the process $\mathcal{Y}_i$ defined as (see Eq. (3) and [11,12])

$$\mathcal{Y}(t) = -\mathrm{j}\int_{-\infty}^{\infty} \mathrm{sign}(\omega) A_{U_i}(\omega, t)\mathrm{e}^{\mathrm{j}\omega t}\mathrm{d}Z(\omega), \quad i = 1, 2, \ldots, n \tag{22}$$

and $A_{U_i}(\omega, t)$ = time–frequency modulating function of the process $U_i(t)$. The following auxiliary state vector process can be defined, similarly to the response processes (see Eq. (12)), as

$$\boldsymbol{\Xi} = \begin{bmatrix} \mathbf{Y} \\ \dot{\mathbf{Y}} \end{bmatrix}_{(2n\times 1)}. \tag{23}$$

Using complex modal decomposition, the cross-covariance matrices of the response processes and the auxiliary processes can be computed as

$$E[\mathbf{Z}(t)\mathbf{Z}^{\mathrm{T}}(t)] = \tilde{\mathbf{T}}^{*} E[\mathbf{S}^{*}(t)\mathbf{S}^{\mathrm{T}}(t)]\tilde{\mathbf{T}}^{T} \tag{24}$$

$$E[\mathbf{Z}(t)\boldsymbol{\Xi}^{\mathrm{T}}(t)] = \tilde{\mathbf{T}}^{*} E[\mathbf{S}^{*}(t)\boldsymbol{\Sigma}^{\mathrm{T}}(t)]\tilde{\mathbf{T}}^{T} \tag{25}$$

where the components of the vector process $\boldsymbol{\Sigma} = [\Sigma_1(t)\, \Sigma_2(t) \cdots \Sigma_{2n}(t)]^{\mathrm{T}}$ are defined as

$$\Sigma_i(t) = -\mathrm{j}\int_{-\infty}^{\infty} \mathrm{sign}(\omega) A_{S_i}(\omega, t)\mathrm{e}^{\mathrm{j}\omega t}\mathrm{d}Z(\omega), \quad i = 1, 2, \ldots, n. \tag{26}$$

Eqs. (24) and (25) show that all quantities in Eq. (21) can be computed from the following spectral characteristics of complex-valued non-stationary processes ($i, m = 1, 2, \ldots, 2n$)

$$\begin{cases} E[S_i^{*}(t)S_m(t)] = \sigma_{S_iS_m}(t) \\ E[S_i^{*}(t)\,\Sigma_m(t)] = \sigma_{S_i\Sigma_m}(t). \end{cases} \tag{27}$$

Notice also that knowledge of the spectral characteristics in Eq. (27) allows computation of the zero-th to second-order spectral characteristics of the components of any vector response quantity $\mathbf{Q}(t)$ linearly related to the displacement response vector $\mathbf{U}(t)$, i.e., $\mathbf{Q}(t) = \mathbf{B}\mathbf{U}(t)$, where $\mathbf{B}$ = constant matrix.

3.3. Response statistics of MDOF linear systems subjected to modulated colored noise

Time-modulated colored noises constitute an important and widely used class of non-stationary dynamic load processes. The expression given in Eq. (18) describing a general non-stationary loading process reduces to

$$F(t) = A_F(t)P(t) \tag{28}$$

where the time-modulating function $A_F(t)$ is frequency-independent and the process $P(t)$ is a colored noise with *PSD* function having the following general expression (i.e., rational function)

$$\Phi_P(\omega) = S_0 \sum_{k=1}^{N} \frac{A_k}{(\omega - \bar{\omega}_k)} \tag{29}$$

where A_k and $\bar{\omega}_k$ ($k = 1, 2, \ldots, N$) = complex-valued constants and S_0 = real-valued scaling constant. In the sequel, it is assumed that the time-modulating functions have the following general expression

$$A_F(t) = H(t) \sum_{q=1}^{M} a_q \mathrm{e}^{b_q t} \tag{30}$$

in which a_q and b_q ($q = 1, 2, \ldots, M$) = real-valued constants, and $H(t)$ = unit-step function.

Substituting Eq. (30) into Eq. (20) yields ($i = 1, 2, \ldots, 2n$)

$$A_{S_i}(\omega, t) = \mathrm{j}\sum_{q=1}^{M} \left\{ a_q \mathrm{e}^{b_q t} \left[\frac{\mathrm{e}^{-\mathrm{j}(\omega - \omega_{iq})t} - 1}{\omega - \omega_{iq}} \right] \right\} \tag{31}$$

where $\omega_i = -\mathrm{j}\lambda_i$ and $\omega_{iq} = \omega_i + \mathrm{j}b_q$. The spectral characteristics defined in Eq. $(27)_1$ can be computed using Cauchy's residue theorem as [19] ($i, m = 1, 2, \ldots, 2n$)

$$\sigma_{S_iS_m}(t) = S_0 \sum_{q=1}^{M}\sum_{s=1}^{M}\sum_{k=1}^{N} a_q a_s A_k \mathrm{e}^{(b_q + b_s)t} \left\{ \left[\mathrm{e}^{\mathrm{j}(\omega_{ms} - \omega^{*}_{iq})t} + 1 \right] \times I_1^{iq,ms,k} - \mathrm{e}^{-\mathrm{j}\omega^{*}_{iq}t} I_2^{iq,ms,k} - \mathrm{e}^{\mathrm{j}\omega_{ms}t} I_3^{iq,ms,k} \right\} \tag{32}$$

in which

$$I_1^{iq,ms,k} = 2\pi\mathrm{j}\sum_{r=1}^{3} B_r^{iq,ms,k} I(\tilde{\omega}_r) \tag{33}$$

$$I_2^{iq,ms,k} = 2\pi\mathrm{j}\sum_{r=1}^{3} B_r^{iq,ms,k} \mathrm{e}^{\mathrm{j}\tilde{\omega}_r t} I(\tilde{\omega}_r) \tag{34}$$

$$I_3^{iq,ms,k} = -2\pi\mathrm{j}\sum_{r=1}^{3} B_r^{iq,ms,k} \mathrm{e}^{-\mathrm{j}\tilde{\omega}_r t} I(-\tilde{\omega}_r) \tag{35}$$

where $\tilde{\omega}_1 = \omega^{*}_{iq}$, $\tilde{\omega}_2 = \omega_{ms}$, $\tilde{\omega}_3 = \bar{\omega}_k$ and

$$B_r^{iq,ms,k} = \frac{1}{(\tilde{\omega}_r - \tilde{\omega}_p)(\tilde{\omega}_r - \tilde{\omega}_q)}, \quad r,p,q = 1,2,3, r \neq p \neq q \quad (36)$$

while

$$I(\omega) = \max\left[\frac{\Im(\omega)}{|\Im(\omega)|}, 0\right] \quad (37)$$

and $\Im(\cdot)$ = imaginary part of the quantity in parentheses. Madsen and Krenk [20] and Krenk and Madsen [21,22] applied the same approach (integration using Cauchy's residue theorem) to the real-valued (second-order) modal responses to derive the closed-form solutions for the auto- and cross-correlation functions of the response processes of classically damped *MDOF* linear systems subjected to white noise excitations modulated by rational time-modulating functions. After extensive algebraic manipulations (see Appendix), the spectral characteristics in Eq. $(27)_2$ are obtained as $(i, m = 1, 2, \ldots, 2n)$

$$\sigma_{S_i\Sigma_m}(t) = -\mathrm{j}S_0 \sum_{q=1}^{M}\sum_{s=1}^{M}\sum_{k=1}^{N} a_q a_s A_k \mathrm{e}^{(b_q+b_s)t}\left\{\left[\mathrm{e}^{\mathrm{j}(\omega_{ms}-\omega_{iq}^*)t}+1\right] \times J_1^{iq,ms,k} - \mathrm{e}^{-\mathrm{j}\omega_{iq}^* t} J_2^{iq,ms,k} - \mathrm{e}^{\mathrm{j}\omega_{ms}t} J_3^{iq,ms,k}\right\} \quad (38)$$

in which

$$J_1^{iq,ms,k} = -\sum_{r=1}^{3}\left\{B_r^{iq,ms,k}\left[\log(\tilde{\omega}_r) + \log(-\tilde{\omega}_r)\right]\right\} \quad (39)$$

$$J_2^{iq,ms,k} = 2\sum_{r=1}^{3} B_r^{iq,ms,k}\left\{\mathrm{e}^{\mathrm{j}\tilde{\omega}_r t}\left[E_1(\mathrm{j}\tilde{\omega}_r t) + \mathrm{j}\pi I(\tilde{\omega}_r)\mathrm{sign}(\Re(\tilde{\omega}_r))\right]\right\} \quad (40)$$

$$J_3^{iq,ms,k} = 2\sum_{r=1}^{3} B_r^{iq,ms,k}\left\{\mathrm{e}^{-\mathrm{j}\tilde{\omega}_r t}\left[E_1(-\mathrm{j}\tilde{\omega}_r t) - \mathrm{j}\pi I(-\tilde{\omega}_r)\mathrm{sign}(\Re(\tilde{\omega}_r))\right]\right\} \quad (41)$$

where $E_1(\cdot)$ denotes the integral exponential function defined as [23]

$$E_1(x) = \int_x^\infty \frac{\mathrm{e}^{-u}}{u}\mathrm{d}u, \quad |\arg(x)| < \pi \quad (42)$$

and $\Re(\cdot)$ = real part of the quantity in parentheses. It is noteworthy that the closed-form exact solutions presented here for the spectral characteristics of MDOF linear system response processes are valid for any kind of time-modulated colored noise excitation as described by Eqs. (28)–(30). On the other hand, the considered description of these response processes includes only first and second order statistical moments and thus is complete only for Gaussian response processes, which are obtained only if the input process is a time-modulated Gaussian colored noise. In the sequel of the paper, only time-modulated Gaussian colored noise excitations are considered.

4. Applications

4.1. Colored noise model

A special important case of colored PSD is

$$\Phi_P(\omega) = \frac{\nu S_0}{2\pi}\left[\frac{1}{\nu^2+(\omega+\eta)^2} + \frac{1}{\nu^2+(\omega-\eta)^2}\right] = \frac{\mathrm{j}S_0}{4\pi}\sum_{k=1}^{4}\left[\frac{(-1)^k}{(\omega-\bar{\omega}_k)}\right] \quad (43)$$

where $\bar{\omega}_1 = -\bar{\omega}_4 = -\eta + \mathrm{j}\nu$, $\bar{\omega}_2 = -\bar{\omega}_3 = -\eta - \mathrm{j}\nu$, and η, ν = parameters defining the shape of the PSD. Eq. (43) is a special case of Eq. (29) with $N = 4$ and $A_k = (-1)^k\mathrm{j}/(4\pi)$, $k = 1, 2, 3, 4$. This

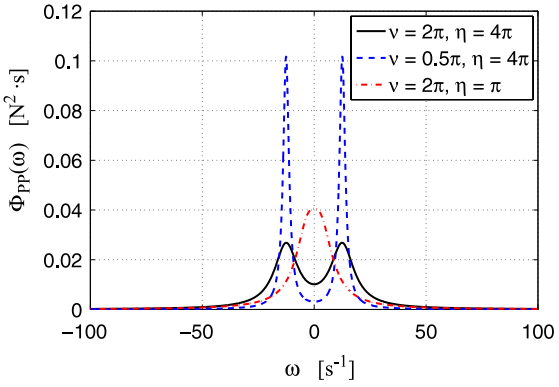

Fig. 1. PSD defined by Eq. (43) for varying values of η and ν.

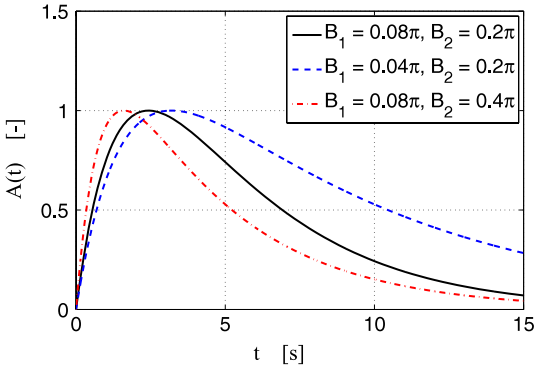

Fig. 2. Shinozuka and Sato's modulating function.

PSD allows representation of extremely different colored noise processes (Fig. 1) and is widely used for earthquake [13] and fluid dynamics applications.

4.2. Modulating function of Shinozuka and Sato

The modulating function of Shinozuka and Sato [24] is defined as

$$A_F(t) = C\left[\mathrm{e}^{-B_1 t} - \mathrm{e}^{-B_2 t}\right]H(t) \quad (44)$$

where

$$C = \left[\frac{B_1}{B_2 - B_1}\right]\mathrm{e}^{\frac{B_2}{B_2-B_1}\log\left(\frac{B_2}{B_1}\right)} \quad (45)$$

and $B_2 > B_1 > 0$. By changing the values of parameters B_1 and $B_2 > 0$, a wide range of different time-modulating functions can be obtained (see Fig. 2). Indeed, the modulating function of Shinozuka and Sato has been used extensively in random vibration studies regarding the computation of probability density distributions of *SDOF* oscillators subjected to non-stationary excitation [25–27]. Using first Eq. (43) as a particular case of Eq. (29) and then Eq. (44) as particular case of Eq. (30), Eq. (38) reduces to $(i, m = 1, 2, \ldots, 2n)$

$$\sigma_{S_i\Sigma_m}(t) = \frac{C^2 S_0}{4\pi}\sum_{q=1}^{2}\sum_{s=1}^{2}\sum_{k=1}^{4}(-1)^{k+s+q}\mathrm{e}^{-(B_q+B_s)t} \times \left\{\left[\mathrm{e}^{\mathrm{j}(\omega_{ms}-\omega_{iq}^*)t}+1\right]J_1^{iq,ms,k} - \mathrm{e}^{-\mathrm{j}\omega_{iq}^* t}J_2^{iq,ms,k} - \mathrm{e}^{\mathrm{j}\omega_{ms}t}J_3^{iq,ms,k}\right\} \quad (46)$$

where $\omega_{iq} = \omega_i - \mathrm{j}B_q$ $(q = 1, 2)$.

4.3. Linear elastic SDOF systems from at rest initial conditions

The first application example consists of a set of linear elastic *SDOF* systems subjected to a Gaussian colored noise given by

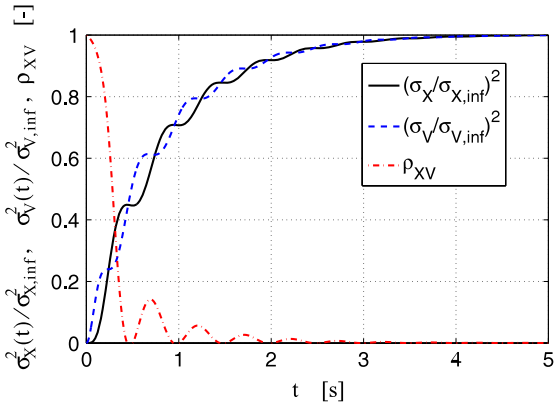

Fig. 3. Normalized displacement and velocity variances and correlation coefficient for a *SDOF* system with natural period $T = 1.0$ s and damping ratio $\xi = 0.10$ subjected to colored white noise ($\eta = 4\pi$, $\nu = 2\pi$) with at rest initial conditions.

Eq. (43) and time-modulated by the unit-step function (i.e., from at rest initial conditions). In this case, the complex modal matrix **T** is given by

$$\mathbf{T} = \begin{bmatrix} 1 & 1 \\ \lambda_1 & \lambda_2 \end{bmatrix} \tag{47}$$

in which

$$\lambda_{1,2} = -\xi\omega_0 \pm \mathrm{j}\omega_d \tag{48}$$

where ξ = viscous damping ratio, ω_0 = natural circular frequency, and $\omega_d = \omega_0\sqrt{1-\xi^2}$ = damped circular frequency of the system. It is assumed that $0 < \xi < 1$, which is usually the case for structural systems. Fig. 3 shows the displacement and velocity response variances (normalized by dividing them by their stationary values) and the correlation coefficient between displacement and velocity response of a linear *SDOF* system with natural period $T = 1.0$ s and damping ratio $\xi = 0.10$. Closed-form solutions for variances and correlation coefficients of several *SDOF* systems with different natural periods and different viscous damping ratios have been verified by Monte Carlo simulation.

For a *SDOF*, the non-geometric spectral characteristic $c_{01,XY}(t) = \sigma_{U\dot{y}}(t)$ can be easily expressed as

$$\sigma_{U\dot{y}}(t) = \frac{\mathrm{j}}{2\omega_d}\sigma_{S_1\Sigma_1}(t). \tag{49}$$

Fig. 4 plots the non-geometric spectral characteristic $c_{01,XY}(t)$ for a linear *SDOF* system with natural period $T = 1.0$ s and different values of the viscous damping ratios ($\xi = 0.01$, 0.05 and 0.10). For comparison purposes, Fig. 4 also shows the Monte Carlo simulation estimates of $c_{01,XY}(t)$. As expected, lower stationary values are reached in a shorter time as the viscous damping ratio increases. It is noteworthy that simulation is very expensive computationally (in this case, 5000 realizations have been used) and simulation results cannot be employed to estimate the bandwidth parameters and central frequencies because of error introduced by the scatter.

Fig. 5 displays the time-variant bandwidth parameter $q(t)$ for the displacement response processes of *SDOF* systems with natural period $T = 1.0$ s and varying damping ratio ($\xi = 0.01$, 0.05 and 0.10) subjected to colored noise with at rest initial conditions. All time-variant bandwidth parameters are equal to one at time $t = 0$ s, which implies that displacement response processes are broad-band at time $t = 0$ s. The displacement response processes become narrow-band for large t. The bandwidth parameter stationary values strongly depend on the damping ratio. The bandwidth parameter time histories are very similar to the case of *SDOF* subjected to white noise with at rest initial conditions [5] but with

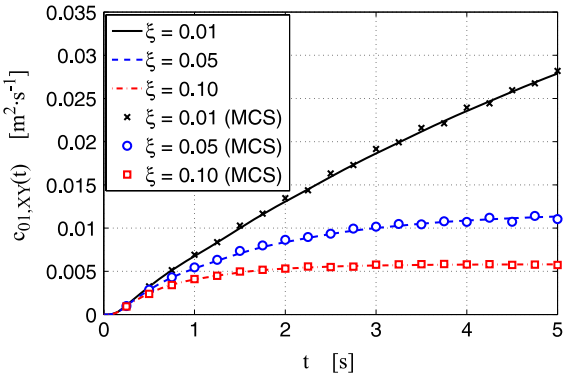

Fig. 4. Comparison of closed-form solutions and Monte Carlo simulations (MCS) of spectral characteristics $c_{01,XY}$ for *SDOF* systems with natural period $T = 1.0$ s and varying damping ratio ($\xi = 0.01$, 0.05 and 0.10) subjected to colored white noise ($\eta = 4\pi$, $\nu = 2\pi$) with at rest initial conditions.

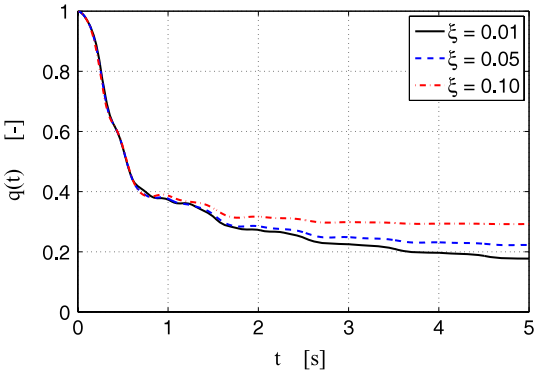

Fig. 5. Time-variant bandwidth parameter $q(t)$ for *SDOF* systems with natural period $T = 1.0$ s and varying damping ratio ($\xi = 0.01$, 0.05 and 0.10) subjected to colored white noise ($\eta = 4\pi$, $\nu = 2\pi$) with at rest initial conditions.

two major differences: (1) for colored excitation, the bandwidth parameter time history depends on the natural period of the *SDOF*, while in the case of white noise excitation, it is possible to express the bandwidth parameter time history as a function of the time normalized by the *SDOF* natural period, and (2) $q(t = 0\text{ s}) = 0.961$ for the displacement response process of a linear *SDOF* system subjected to white noise, while $q(t = 0\text{ s}) = 1.000$ for the displacement response process of a linear *SDOF* system subjected to colored noise (see Fig. 5). Fig. 6 shows the ratio of the central frequency of the displacement response process over the natural circular frequency, referred to as the normalized central frequency, of *SDOF* systems with natural period $T = 1.0$ s and varying damping ratio ($\xi = 0.01$, 0.05 and 0.10). It is observed that: (1) The normalized central frequency has a very high value for small t, then as t increases it reaches a minimum and finally oscillates until it reaches stationarity. Differently from *SDOF* systems subjected to white noise excitation, these oscillations do not necessarily remain below the value of the natural circular frequency. (2) The normalized central frequency is a function of both damping ratio and natural period T of the *SDOF* system. Differently from *SDOF* systems subjected to white noise excitation, the stationary value of the normalized central frequency is not independent of T.

It is noteworthy that Eq. (49) can be directly employed for computing the corresponding first-order *NGSCs* of the response processes of linear *MDOF* systems that are classically damped, by using real-valued (second-order) mode superposition and thus avoiding complex modal analysis, which is computationally more expensive and less commonly used. As a consequence, the time-variant bandwidth parameter and central frequency of classically damped linear *MDOF* systems can also be computed very efficiently.

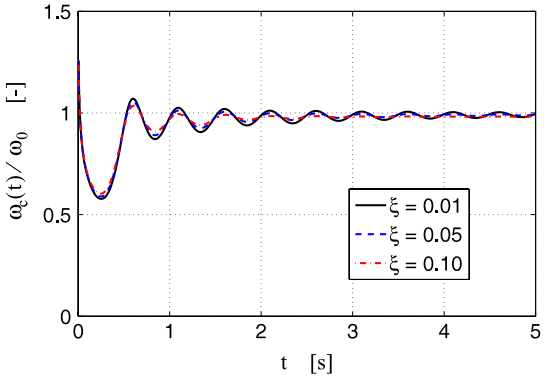

Fig. 6. Time-variant central frequency $\omega_c(t)$ for *SDOF* systems with natural period $T = 1.0$ s and varying damping ratio ($\xi = 0.01$, 0.05 and 0.10) subjected to colored white noise ($\eta = 4\pi$, $\nu = 2\pi$) with at rest initial conditions.

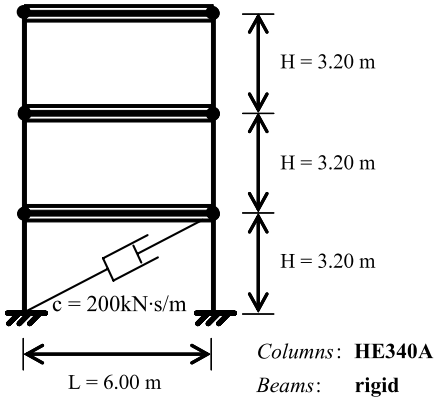

Fig. 7. Geometric configuration of benchmark three-storey one-bay shear-type steel frame.

4.4. Three-storey shear-type building (linear MDOF system)

The three-storey one-bay steel shear-frame shown in Fig. 7 is considered as an application example. This building structure has a uniform storey height $H = 3.20$ m and a bay width $L = 6.00$ m. The steel columns are made of European *HE*340*A* wide flange beams with moment of inertia along the strong axis $I = 27690.0$ cm^4. The steel material is modeled as linear elastic with Young's modulus $E = 200$ GPa. The beams are considered rigid to enforce a typical shear building behavior. Under this assumptions, the shear-frame is modeled as a 3-*DOF* linear system.

The frame described above is assumed to be part of a building structure with a distance between frames $L' = 6.00$ m. The tributary mass per storey, M, is obtained assuming a distributed gravity load of $q = 8$ kN/m^2, accounting for the structure's own weight, as well as for permanent and live loads, and is equal to $M = 28800$ kg. The modal periods of the linear elastic undamped shear-frame are $T_1 = 0.38$ s, $T_2 = 0.13$ s and $T_3 = 0.09$ s, with corresponding effective modal mass ratios of 91.41%, 7.49% and 1.10%, respectively. Viscous damping in the form of Rayleigh damping is assumed with a damping ratio $\xi = 0.02$ for the first and third modes of vibration. The same shear-frame is also considered with the addition of a viscous damper of coefficient $c = 200$ kN s/m across the first storey as shown in Fig. 7. The structure with a viscous damper is a non-classically damped system.

Both classically and non-classically damped systems are subjected to the same stochastic ground motion input. The earthquake ground acceleration is modeled as a non-stationary stochastic process described by the colored noise PSD given in Eq. (43) time-modulated by the Shinozuka and Sato's modulating function (Eq. (45)). The parameters defining the colored noise are

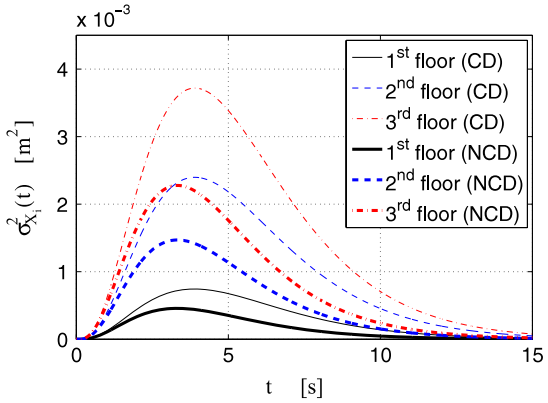

Fig. 8. Time-variant time histories of the floor relative displacement variances for both classically (without viscous damper: CD) and non-classically (with viscous damper: NCD) damped structures.

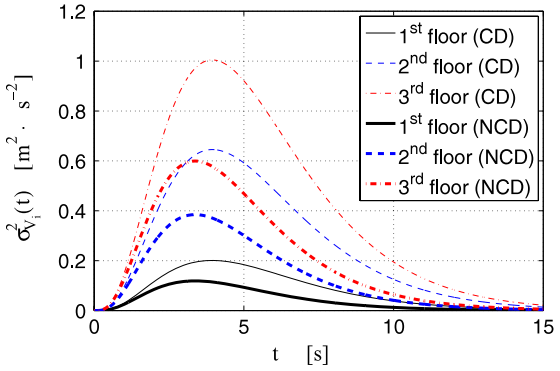

Fig. 9. Time-variant time histories of the floor relative velocity variances for both classically (without viscous damper: CD) and non-classically (with viscous damper: NCD) damped structures.

assumed as $\nu = 2\pi$ rad/s, $\eta = 4\pi$ rad/s and $S_0 = 10$ m^2/s^3. The parameters defining the modulating function are taken as $B_1 = 0.08\pi$ and $B_2 = 0.20\pi$. The modulating function reaches its peak value at time $T_{peak} = 2.43$ s.

Figs. 8–11 show the time histories of (1) the variances of the floor displacements relative to ground (in short, relative displacements), (2) variances of the floor velocities relative to ground (in short, relative velocities), (3) bandwidth parameters, and (4) central frequencies (normalized by the first mode natural frequency) of the floor relative displacement responses. All quantities are provided for both the classically (i.e., without damper) and non-classically damped case. All presented closed-form solutions have been verified by Monte Carlo simulation. Figs. 8 and 9 show that in the non-classically damped case, compared to the classically damped case, (1) the peak values of both relative displacement and velocity variances reduce significantly, (2) the peak values of these variances are reached earlier, and (3) the variance time histories have a shape very similar to the shape of the time-modulating function.

Figs. 10 and 11 show that the floor relative displacement response processes are dominated, as expected, by the first mode contribution and thus vary very little among first, second and third floors. The normalized central frequency stationary values are all very close to one. Figs. 10 and 11 also provide a zoom view of the first 0.4 s of the time history of the bandwidth parameters and central frequencies, respectively, of the three floor's relative displacements. These zoom views show that the spectral properties of the displacement response processes for the second and third floor of the considered system are very similar for both the classically and non-classically damped structural model.

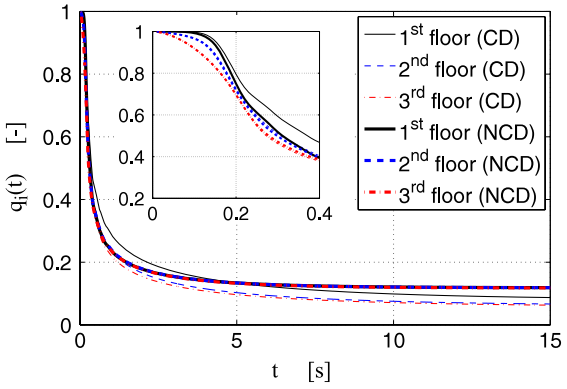

Fig. 10. Time-variant bandwidth parameter of the floor relative displacement processes for both classically (without viscous damper: CD) and non-classically (with viscous damper: NCD) damped structures.

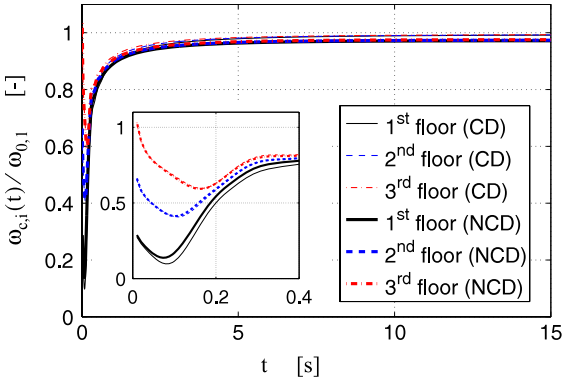

Fig. 11. Time-variant central frequency (normalized by the first mode natural circular frequency) of the floor relative displacement processes for both classically (without viscous damper: CD) and non-classically (with viscous damper: NCD) damped structures.

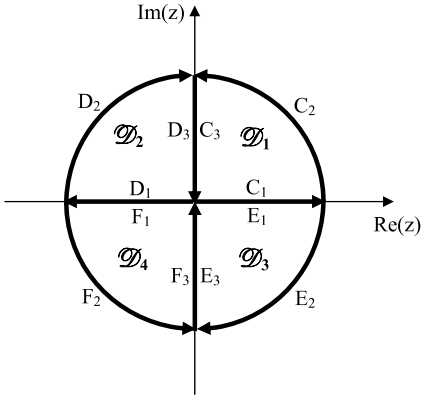

Fig. 12. Integration paths and domains for integrals with exponentials.

Small but non-negligible differences between classically and non-classically damped systems are observed in the spectral properties (i.e., bandwidth parameter and central frequency) of the first storey relative displacement response process.

This second application example illustrates the capability of the presented extension of non-geometric spectral characteristics to complex-valued stochastic processes to capture the time-variant spectral properties in terms of the bandwidth parameter and central frequency of the response of linear *MDOF* classically and non-classically damped systems.

5. Conclusions

This paper presents new closed-form exact solutions for the non-geometric spectral characteristics (*NGSCs*) of general complex-valued non-stationary random processes. These newly defined *NGSCs* are essential for computing the time-variant bandwidth parameter and central frequency of non-stationary response processes of linear systems. The bandwidth parameter is also used in structural reliability applications, e.g., for obtaining analytical approximations of the probability that a structural response process out-crosses a specified limit-state threshold. Closed-form exact solutions are derived and presented for the time-variant bandwidth parameter and central frequency of non-stationary response processes of linear *SDOF* and *MDOF* systems subjected to time-modulated Gaussian colored noise excitations. All the presented closed-form solutions are validated through Monte Carlo simulation.

The obtained exact closed-form solutions have direct and important applications, since the response of many structures can be approximated by using linear *SDOF* and *MDOF* models, and provide valuable benchmark solutions for validating (at the linear structural response level) numerical methods developed to estimate the probabilistic response of non-linear systems subjected to non-stationary excitations. More general models for the time-variant excitation are also the object of ongoing research by the authors.

Acknowledgements

Support of this research by the LSU Council on Research through the 2008 Summer Stipend Program and the Louisiana Board of Regents through the Pilot Funding for New Research (Pfund) Program of the National Science Foundation (NSF) Experimental Program to Stimulate Competitive Research (EPSCoR) under Award No. NSF(2008)-PFUND86 is gratefully acknowledged. Any opinions, findings, and conclusions or recommendations expressed in this material are those of the authors and do not necessarily reflect those of the sponsors.

Appendix

The evaluation via Cauchy's residual method of the integrals appearing in Eq. (38) is here reported. Integration paths and integration domains for the relevant integrals are shown in the complex plane in Fig. 12.

$$
\begin{aligned}
J_1^{iq,ms,k} &= \int_{-\infty}^{\infty} \frac{\operatorname{sign}(\omega)}{(\omega-\tilde{\omega}_1)(\omega-\tilde{\omega}_2)(\omega-\tilde{\omega}_3)}\mathrm{d}\omega \\
&= \sum_{r=1}^{3} B_r^{iq,ms,k} \int_{-\infty}^{\infty} \frac{\operatorname{sign}(\omega)}{(\omega-\tilde{\omega}_r)}\mathrm{d}\omega \\
&= \sum_{r=1}^{3} B_r^{iq,ms,k} \left[\int_0^{\infty} \frac{1}{(\omega-\tilde{\omega}_r)}\mathrm{d}\omega + \int_0^{\infty} \frac{1}{(\omega+\tilde{\omega}_r)}\mathrm{d}\omega\right] \\
&= \sum_{r=1}^{3} B_r^{iq,ms,k} \left\{\lim_{\omega\to\infty} \log\left[(\omega-\tilde{\omega}_r)(\omega+\tilde{\omega}_r)\right]\right. \\
&\quad \left. - \log(\tilde{\omega}_r) - \log(-\tilde{\omega}_r)\right\} \\
&= \lim_{\omega\to\infty} \left[\log(\omega^2-\tilde{\omega}_r^2)^{\sum_{r=1}^{3} B_r^{iq,ms,k}}\right] \\
&\quad - \sum_{r=1}^{3} B_r^{iq,ms,k} \left[\log(\tilde{\omega}_r) + \log(-\tilde{\omega}_r)\right] \\
&= -\sum_{r=1}^{3} B_r^{iq,ms,k} \left[\log(\tilde{\omega}_r) + log(-\tilde{\omega}_r)\right] \qquad (50)
\end{aligned}
$$

where the relations $\sum_{r=1}^{3} B_r^{iq,ms,k} = 0, x^0 = 1$ (x real number) and $\log 1 = 0$ are used.

$$J_2^{iq,ms,k} = \int_{-\infty}^{\infty} \frac{\operatorname{sign}(\omega)\mathrm{e}^{\mathrm{j}\omega t}}{(\omega-\tilde{\omega}_1)(\omega-\tilde{\omega}_2)(\omega-\tilde{\omega}_3)}\mathrm{d}\omega = \sum_{r=1}^{3} B_r^{iq,ms,k}\int_{-\infty}^{\infty}\frac{\operatorname{sign}(\omega)\mathrm{e}^{\mathrm{j}\omega t}}{(\omega-\tilde{\omega}_r)}\mathrm{d}\omega = \sum_{r=1}^{3} B_r^{iq,ms,k}\left[\int_0^{\infty}\frac{\mathrm{e}^{\mathrm{j}\omega t}}{(\omega-\tilde{\omega}_r)}\mathrm{d}\omega - \int_{-\infty}^{0}\frac{\mathrm{e}^{\mathrm{j}\omega t}}{(\omega-\tilde{\omega}_r)}\mathrm{d}\omega\right] \quad (51)$$

$$\begin{aligned} I_C &= \oint \frac{\mathrm{e}^{\mathrm{j}zt}}{(z-\tilde{\omega}_r)}\mathrm{d}z \\ &= \oint_{C_1}\frac{\mathrm{e}^{\mathrm{j}zt}}{(z-\tilde{\omega}_r)}\mathrm{d}z + \oint_{C_2}\frac{\mathrm{e}^{\mathrm{j}zt}}{(z-\tilde{\omega}_r)}\mathrm{d}z + \oint_{C_3}\frac{\mathrm{e}^{\mathrm{j}zt}}{(z-\tilde{\omega}_r)}\mathrm{d}z \\ &= I_{C_1} + I_{C_2} + I_{C_3} \end{aligned} \quad (52)$$

$$\begin{aligned} I_C &= 2\mathrm{j}\pi\operatorname{Res}_{\tilde{\omega}_r\in\mathcal{D}_1}[\mathrm{e}^{\mathrm{j}zt},\tilde{\omega}_r] \\ &= 2\mathrm{j}\pi\mathrm{e}^{\mathrm{j}\tilde{\omega}_r t} I(\tilde{\omega}_r)R(\tilde{\omega}_r) \end{aligned} \quad (53)$$

where

$$R(\omega) = \max\left[\frac{\Re(\omega)}{|\Re(\omega)|}, 0\right] \quad (54)$$

$$I_{C_1} = \int_0^{\infty}\frac{\mathrm{e}^{\mathrm{j}\omega t}}{(\omega-\tilde{\omega}_r)}\mathrm{d}\omega \quad (55)$$

$$\begin{aligned} I_{C_2} &= \lim_{R\to\infty}\int_0^{\frac{\pi}{2}}\frac{\mathrm{e}^{\mathrm{j}R\mathrm{e}^{\mathrm{j}\theta}t}}{(R\mathrm{e}^{\mathrm{j}\theta}-\tilde{\omega}_r)}R\mathrm{j}\mathrm{e}^{\mathrm{j}\theta}\mathrm{d}\theta \\ &= \mathrm{j}\lim_{R\to\infty}\int_0^{\frac{\pi}{2}}\mathrm{e}^{\mathrm{j}Rt\cos\theta}\mathrm{e}^{-Rt\sin\theta}\mathrm{d}\theta = 0 \end{aligned} \quad (56)$$

$$\begin{aligned} I_{C_3} &= \mathrm{j}\int_{\infty}^{0}\frac{\mathrm{e}^{-xt}}{\mathrm{j}x-\tilde{\omega}_r}\mathrm{d}x = -\int_0^{\infty}\frac{\mathrm{e}^{-xt}}{x+\mathrm{j}\tilde{\omega}_r}\mathrm{d}x \\ &= -\mathrm{e}^{\mathrm{j}\tilde{\omega}_r t}\int_{\mathrm{j}\tilde{\omega}_r}^{\infty}\frac{\mathrm{e}^{-(x+\mathrm{j}\tilde{\omega}_r)t}}{x+\mathrm{j}\tilde{\omega}_r}\mathrm{d}(x+\mathrm{j}\tilde{\omega}_r) \\ &= -\mathrm{e}^{\mathrm{j}\tilde{\omega}_r t}\int_{\mathrm{j}\tilde{\omega}_r t}^{\infty}\frac{\mathrm{e}^{-u}}{u}\mathrm{d}u = -\mathrm{e}^{\mathrm{j}\tilde{\omega}_r t}E_1(\mathrm{j}\tilde{\omega}_r t) \end{aligned} \quad (57)$$

$$\begin{aligned} I_{C_1} &= I_C - I_{C_2} - I_{C_3} \\ &= \mathrm{e}^{\mathrm{j}\tilde{\omega}_r t}\left[2\mathrm{j}\pi I(\tilde{\omega}_r)R(\tilde{\omega}_r) + E_1(\mathrm{j}\tilde{\omega}_r t)\right] \end{aligned} \quad (58)$$

$$\begin{aligned} I_D &= \oint_D \frac{\mathrm{e}^{\mathrm{j}zt}}{z-\tilde{\omega}_r}\mathrm{d}z \\ &= \oint_{D_1}\frac{\mathrm{e}^{\mathrm{j}zt}}{z-\tilde{\omega}_r}\mathrm{d}z + \oint_{D_2}\frac{\mathrm{e}^{\mathrm{j}zt}}{z-\tilde{\omega}_r}\mathrm{d}z + \oint_{D_3}\frac{\mathrm{e}^{\mathrm{j}zt}}{z-\tilde{\omega}_r}\mathrm{d}z \\ &= I_{D_1} + I_{D_2} + I_{D_3} \end{aligned} \quad (59)$$

$$\begin{aligned} I_D &= -2\mathrm{j}\pi\operatorname{Res}_{\tilde{\omega}_r\in\mathcal{D}_2}[\mathrm{e}^{\mathrm{j}zt},\tilde{\omega}_r] \\ &= -2\mathrm{j}\pi\mathrm{e}^{\mathrm{j}\tilde{\omega}_r t}I(\tilde{\omega}_r)R(-\tilde{\omega}_r) \end{aligned} \quad (60)$$

$$I_{D_1} = \int_0^{-\infty}\frac{\mathrm{e}^{\mathrm{j}\omega t}}{(\omega-\tilde{\omega}_r)}\mathrm{d}\omega = -\int_{-\infty}^{0}\frac{\mathrm{e}^{\mathrm{j}\omega t}}{(\omega-\tilde{\omega}_r)}\mathrm{d}\omega \quad (61)$$

$$\begin{aligned} I_{D_2} &= \lim_{R\to\infty}\int_{\pi}^{\frac{\pi}{2}}\frac{\mathrm{e}^{\mathrm{j}R\mathrm{e}^{\mathrm{j}\theta}t}}{(R\mathrm{e}^{\mathrm{j}\theta}-\tilde{\omega}_r)}R\mathrm{j}\mathrm{e}^{\mathrm{j}\theta}\mathrm{d}\theta \\ &= \mathrm{j}\lim_{R\to\infty}\int_{\pi}^{\frac{\pi}{2}}\mathrm{e}^{\mathrm{j}Rt\cos\theta}\mathrm{e}^{-Rt\sin\theta}\mathrm{d}\theta = 0 \end{aligned} \quad (62)$$

$$\begin{aligned} I_{D_3} &= \mathrm{j}\int_{\infty}^{0}\frac{\mathrm{e}^{-xt}}{\mathrm{j}x-\tilde{\omega}_r}\mathrm{d}x = -\int_0^{\infty}\frac{\mathrm{e}^{-xt}}{x+\mathrm{j}\tilde{\omega}_r}\mathrm{d}x \\ &= -\mathrm{e}^{\mathrm{j}\tilde{\omega}_r t}E_1(\mathrm{j}\tilde{\omega}_r t) \end{aligned} \quad (63)$$

$$\begin{aligned} I_{D_1} &= I_D - I_{D_2} - I_{D_3} \\ &= \mathrm{e}^{\mathrm{j}\tilde{\omega}_r t}\left[-2\mathrm{j}\pi I(\tilde{\omega}_r)R(-\tilde{\omega}_r) + E_1(\mathrm{j}\tilde{\omega}_r t)\right] \end{aligned} \quad (64)$$

$$J_2^{iq,ms,k} = \sum_{r=1}^{3} B_r^{iq,ms,k}(I_{C_1} + I_{D_1}) = 2\sum_{r=1}^{3} B_r^{iq,ms,k}\left\{\mathrm{e}^{\mathrm{j}\tilde{\omega}_r t}\left[E_1(\mathrm{j}\tilde{\omega}_r t) + \mathrm{j}\pi I(\tilde{\omega}_r)\operatorname{sign}(\Re(\tilde{\omega}_r))\right]\right\} \quad (65)$$

$$J_3^{iq,ms,k} = \int_{-\infty}^{\infty}\frac{\operatorname{sign}(\omega)\mathrm{e}^{-\mathrm{j}\omega t}}{(\omega-\tilde{\omega}_1)(\omega-\tilde{\omega}_2)(\omega-\tilde{\omega}_3)}\mathrm{d}\omega = \sum_{r=1}^{3} B_r^{iq,ms,k}\int_{-\infty}^{\infty}\frac{\operatorname{sign}(\omega)\mathrm{e}^{-\mathrm{j}\omega t}}{(\omega-\tilde{\omega}_r)}\mathrm{d}\omega = \sum_{r=1}^{3} B_r^{iq,ms,k}\left[\int_0^{\infty}\frac{\mathrm{e}^{-\mathrm{j}\omega t}}{(\omega-\tilde{\omega}_r)}\mathrm{d}\omega - \int_{-\infty}^{0}\frac{\mathrm{e}^{-\mathrm{j}\omega t}}{(\omega-\tilde{\omega}_r)}\mathrm{d}\omega\right] \quad (66)$$

$$\begin{aligned} I_E &= \oint_E \frac{\mathrm{e}^{-\mathrm{j}zt}}{z-\tilde{\omega}_r}\mathrm{d}z \\ &= \oint_{E_1}\frac{\mathrm{e}^{-\mathrm{j}zt}}{z-\tilde{\omega}_r}\mathrm{d}z + \oint_{E_2}\frac{\mathrm{e}^{-\mathrm{j}zt}}{z-\tilde{\omega}_r}\mathrm{d}z + \oint_{E_3}\frac{\mathrm{e}^{-\mathrm{j}zt}}{z-\tilde{\omega}_r}\mathrm{d}z \\ &= I_{E_1} + I_{E_2} + I_{E_3} \end{aligned} \quad (67)$$

$$\begin{aligned} I_E &= -2\mathrm{j}\pi\operatorname{Res}_{\tilde{\omega}_r\in\mathcal{D}_3}[\mathrm{e}^{-\mathrm{j}zt},\tilde{\omega}_r] \\ &= -2\mathrm{j}\pi\mathrm{e}^{-\mathrm{j}\tilde{\omega}_r t}I(-\tilde{\omega}_r)R(\tilde{\omega}_r) \end{aligned} \quad (68)$$

$$I_{E_1} = \int_0^{\infty}\frac{\mathrm{e}^{-\mathrm{j}\omega t}}{(\omega-\tilde{\omega}_r)}\mathrm{d}\omega \quad (69)$$

$$\begin{aligned} I_{E_2} &= \lim_{R\to\infty}\int_0^{-\frac{\pi}{2}}\frac{\mathrm{e}^{-\mathrm{j}R\mathrm{e}^{\mathrm{j}\theta}t}}{(R\mathrm{e}^{\mathrm{j}\theta}-\tilde{\omega}_r)}R\mathrm{j}\mathrm{e}^{\mathrm{j}\theta}\mathrm{d}\theta \\ &= \mathrm{j}\lim_{R\to\infty}\int_0^{-\frac{\pi}{2}}\mathrm{e}^{-\mathrm{j}Rt\cos\theta}\mathrm{e}^{Rt\sin\theta}\mathrm{d}\theta = 0 \end{aligned} \quad (70)$$

$$\begin{aligned} I_{E_3} &= \mathrm{j}\int_{-\infty}^{0}\frac{\mathrm{e}^{xt}}{\mathrm{j}x-\tilde{\omega}_r}\mathrm{d}x = -\int_0^{-\infty}\frac{\mathrm{e}^{xt}}{x+\mathrm{j}\tilde{\omega}_r}\mathrm{d}x \\ &= -\mathrm{e}^{-\mathrm{j}\tilde{\omega}_r t}E_1(-\mathrm{j}\tilde{\omega}_r t) \end{aligned} \quad (71)$$

$$\begin{aligned} I_{E_1} &= I_E - I_{E_2} - I_{E_3} \\ &= \mathrm{e}^{-\mathrm{j}\tilde{\omega}_r t}\left[-2\mathrm{j}\pi I(-\tilde{\omega}_r)R(\tilde{\omega}_r) + E_1(-\mathrm{j}\tilde{\omega}_r t)\right] \end{aligned} \quad (72)$$

$$\begin{aligned} I_F &= \oint_F \frac{\mathrm{e}^{-\mathrm{j}zt}}{z-\tilde{\omega}_r}\mathrm{d}z \\ &= \oint_{F_1}\frac{\mathrm{e}^{-\mathrm{j}zt}}{z-\tilde{\omega}_r}\mathrm{d}z + \oint_{F_2}\frac{\mathrm{e}^{-\mathrm{j}zt}}{z-\tilde{\omega}_r}\mathrm{d}z + \oint_{F_3}\frac{\mathrm{e}^{-\mathrm{j}zt}}{z-\tilde{\omega}_r}\mathrm{d}z \\ &= I_{F_1} + I_{F_2} + I_{F_3} \end{aligned} \quad (73)$$

$$\begin{aligned} I_F &= 2\mathrm{j}\pi\operatorname{Res}_{\tilde{\omega}_r\in\mathcal{D}_4}[\mathrm{e}^{-\mathrm{j}zt},\tilde{\omega}_r] \\ &= 2\mathrm{j}\pi\mathrm{e}^{-\mathrm{j}\tilde{\omega}_r t}I(-\tilde{\omega}_r)R(-\tilde{\omega}_r) \end{aligned} \quad (74)$$

$$I_{F_1} = \int_0^{-\infty}\frac{\mathrm{e}^{-\mathrm{j}\omega t}}{(\omega-\tilde{\omega}_r)}\mathrm{d}\omega = -\int_{-\infty}^{0}\frac{\mathrm{e}^{-\mathrm{j}\omega t}}{(\omega-\tilde{\omega}_r)}\mathrm{d}\omega \quad (75)$$

$$\begin{aligned} I_{F_2} &= \lim_{R\to\infty}\int_{-\pi}^{-\frac{\pi}{2}}\frac{\mathrm{e}^{-\mathrm{j}R\mathrm{e}^{\mathrm{j}\theta}t}}{(R\mathrm{e}^{\mathrm{j}\theta}-\tilde{\omega}_r)}R\mathrm{j}\mathrm{e}^{\mathrm{j}\theta}\mathrm{d}\theta \\ &= \mathrm{j}\lim_{R\to\infty}\int_{-\pi}^{-\frac{\pi}{2}}\mathrm{e}^{-\mathrm{j}Rt\cos\theta}\mathrm{e}^{Rt\sin\theta}\mathrm{d}\theta = 0 \end{aligned} \quad (76)$$

$$I_{F_3} = \mathrm{j}\int_{-\infty}^{0}\frac{\mathrm{e}^{xt}}{\mathrm{j}x-\tilde{\omega}_r}\mathrm{d}x = -\mathrm{e}^{-\mathrm{j}\tilde{\omega}_r t}E_1(-\mathrm{j}\tilde{\omega}_r t) \quad (77)$$

$$\begin{aligned} I_{F_1} &= I_F - I_{F_2} - I_{F_3} \\ &= \mathrm{e}^{-\mathrm{j}\tilde{\omega}_r t}\left[2\mathrm{j}\pi I(-\tilde{\omega}_r)R(-\tilde{\omega}_r) + E_1(-\mathrm{j}\tilde{\omega}_r t)\right] \end{aligned} \quad (78)$$

$$J_3^{iq,ms,k} = \sum_{r=1}^{3} B_r^{iq,ms,k}(I_{E_1} + I_{F_1}) = 2\sum_{r=1}^{3} B_r^{iq,ms,k}\left\{e^{-j\tilde{\omega}_r t}\left[E_1(-j\tilde{\omega}_r t) - j\pi I(-\tilde{\omega}_r)\mathrm{sign}(\Re(\tilde{\omega}_r))\right]\right\}. \quad (79)$$

References

[1] Priestley MB. Spectral analysis and time series, Univariate series, Multivariate series, prediction and control, fifth printing. vols. 1, 2. London (UK): Academic Press; 1987.
[2] Nigam NC. Introduction to random vibrations. Cambridge (USA): MIT Press; 1983.
[3] Di Paola M. Transient spectral moments of linear systems. SM Archives 1985; 10:225–43.
[4] Michaelov G, Sarkani S, Lutes LD. Spectral characteristics of nonstationary random processes—A critical review. Structural Safety 1999;21:223–44.
[5] Barbato M, Conte JP. Spectral characteristics of non-stationary random processes: Theory and applications to linear structural models. Probabilistic Engineering Mechanics 2008;23:416–26.
[6] Corotis RB, Vanmarcke EH, Cornell CA. First passage of nonstationary random processes. Journal of Engineering Mechanics Division, ASME 1972;98(EM2): 401–14.
[7] Spanos PTD. Spectral moment calculation of linear system output. Journal of Applied Mechanics, ASME 1983;50(12):901–3.
[8] Spanos PTD, Miller SM. Hilbert transform generalization of a classical random vibration integral. Journal of Applied Mechanics, ASME 1994;61(9):575–81.
[9] Crandall SH. First-crossing probabilities of the linear oscillator. Journal of Sound and Vibration 1970;12(3):285–99.
[10] Barbato M, Conte JP. Extension of spectral characteristics to complex-valued random processes and applications in structural reliability. In: Proceedings. ICASP10. 2007.
[11] Arens R. Complex processes for envelopes of normal noise. IRE Transactions on Information Theory 1957;3:204–7.
[12] Dugundji J. Envelope and pre-envelope of real waveforms. IRE Transactions on Information Theory 1958;4:53–7.
[13] Peng B-F, Conte JP. Closed-form solutions for the response of linear systems to fully nonstationary earthquake excitation. Journal of Engineering Mechanics, ASCE 1998;124(6):684–94.
[14] Rice SO. Mathematical analysis of random noise. Bell System Technical Journal 1944;23:282–332.
[15] Rice SO. Mathematical analysis of random noise. Bell System Technical Journal 1945;24:146–56.
[16] Vanmarcke EH. On the distribution of the first-passage time for normal stationary random processes. Journal of Applied Mechanics, ASME 1975;42: 215–20.
[17] Lin YK. Probabilistic theory of structural dynamics. New York (NY): McGraw-Hill; 1967 [Huntington (UK): Krieger Pub., 1976].
[18] Reid JG. Linear system fundamentals: Continuous and discrete, classic and modern. New York (USA): McGraw-Hill; 1983.
[19] Barbato M, Conte JP. Spectral characteristics of non-stationary stochastic processes: Theory and applications to linear structural systems. Report SSR-07-23. La Jolla (CA): University of California at San Diego; 2007.
[20] Madsen PH, Krenk S. Stationary and transient response statistics. Journal of the Engineering Mechanics Division, ASCE 1982;108(EM4):622–34.
[21] Krenk S, Madsen HO, Madsen PH. Stationary and transient response envelopes. Journal of Engineering Mechanics, ASCE 1983;109(1):263–78.
[22] Krenk S, Madsen PH. Stochastic response analysis. In: Thoft-Christensen P, Martinus Nijhoff, editors. NATO ASI series: Reliability theory and its application in structural and soil mechanics, 1983. p. 103–72.
[23] Abramowitz M, Stegun IA. Exponential integral and related functions. In: Handbook of mathematical functions with formulas, graphs, and mathematical tables. 9th printing. New York (USA): Dover; 1972. p. 227–33 [Chapter 5].
[24] Shinozuka M, Sato Y. Simulation of nonstationary random processes. Journal of the Engineering Mechanics Division, ASCE 1967;93(EM1):11–40.
[25] Solomos GP, Spanos PTD. Structural reliability under evolutionary seismic excitation. Soil Dynamics and Earthquake Engineering 1983;2:110–6.
[26] Spanos PTD, Solomos GP. Barrier crossing due to transient excitation. Journal of Engineering Mechanics, ASCE 1984;110(1):20–36.
[27] Spanos PTD, Solomos GP. Oscillator response to nonstationary excitation. Journal of Applied Mechanics, ASME 1984;51(4):907–12.